Published in final edited form as:

Mol Neurobiol. 2018 December ; 55(12): 9057–9074. doi:10.1007/s12035-018-1046-4.

Elevated MeCP2 in Mice Causes Neurodegeneration Involving Tau Dysregulation and Excitotoxicity: Implications for the Understanding and Treatment of MeCP2 Triplication Syndrome

Kristen R. Montgomery[1], **A. S. C. Louis Sam Titus**[1], **Lulu Wang**[1], and **Santosh R. D'Mello**[1]

[1]Department of Biological Sciences, Southern Methodist University, 6501 Airline Drive, Dallas, TX 75275, USA

Abstract

Expression of MeCP2 must be carefully regulated as a reduction or increase results in serious neurological disorders. We are studying transgenic mice in which the MeCP2 gene is expressed at about three times higher than the normal level. Male MeCP2- Tg mice, but not female mice, suffer motor and cognitive deficits and die at 18–20 weeks of age. MeCP2-Tg mice display elevated GFAP and Tau expression within the hippocampus and cortex followed by neuronal loss in these brain regions. Loss of Purkinje neurons, but not of granule neurons in the cerebellar cortex is also seen. Exposure of cultured cortical neurons to either conditioned medium from astrocytes (ACM) derived from male MeCP2-Tg mice or normal astrocytes in which MeCP2 is expressed at elevated levels promotes their death. Interestingly, ACM from male, but not female MeCP2-Tg mice, displays this neurotoxicity reflecting the gender selectivity of neurological symptoms in mice. Male ACM, but not female ACM, contains highly elevated levels of glutamate, and its neurotoxicity can be prevented by MK-801, indicating that it is caused by excitotoxicity. Based on the close phenotypic resemblance of MeCP2-Tg mice to patients with *MECP2* triplication syndrome, we suggest for the first time that the human syndrome is a neurodegenerative disorder resulting from astrocyte dysfunction that leads to Tau-mediated excitotoxic neurodegeneration. Loss of cortical and hippocampal neurons may explain the mental retardation and epilepsy in patients, whereas ataxia likely results from the loss of Purkinje neurons.

Keywords

MeCP2 triplication syndrome; Tau; GFAP; Astrocyte dysfunction; Neurodegeneration

Introduction

Methyl-CpG-binding protein 2 (MeCP2) is a protein that binds to methylated DNA and regulates chromatin structure, transcription, and splicing [1–3]. Although ubiquitously expressed, MeCP2 is most abundantly produced in the brain where it is expressed primarily

Correspondence to: Santosh R. D'Mello.

Kristen R. Montgomery and A. S. C. Louis Sam Titus contributed equally to this work.

Electronic supplementary material The online version of this article (https://doi.org/10.1007/s12035-018-1046-4) contains supplementary material, which is available to authorized users.

in postmitotic neurons. The role of MeCP2 in neuronal or brain function is not well understood and the subject of intense investigation [2,4]. Loss of MeCP2 function causes Rett syndrome, a neurodevelopmental disorder primarily affecting females (because the gene is X-linked) [5, 6]. Unexpectedly, increased MeCP2 expression resulting from gene duplication or triplication causes a different and more severe neurological disorder called *MECP2* duplication or *MECP2* triplication syndrome ([7–9]). Males with this syndrome display severe mental retardation, motor deficits, epilepsy, progressive spasticity, and premature death. Macrocephaly is observed in more severe cases of *MECP2* duplication syndrome and with *MECP2* gene triplication [7–10]. Non-neurological symptoms include constipation and recurrent infections [8–10]. Females with *MECP2* gene triplications are often asymptomatic due to highly skewed X-chromosome inactivation. MRI scans of affected patients have revealed generalized cortical atrophy, loss of white matter, and mildly enlarged lateral ventricles indicating neuronal loss [9, 11, 12]. In one case where results of postmortem neuropathological analysis have been reported, diffuse neuronal loss in the cortex and minor disturbance of cortical lamination was observed [13].

We have been studying a transgenic mouse line, MeCP2- Tg3, generated by Collins et al. in which the human *MECP2* transgene is localized to the X chromosome and expressed from its own promoter [14]. The transgenic mice, henceforth referred to as MeCP2-Tg mice, express MeCP2 at about 3-fold higher than normal levels. Female transgenic mice appear normal while male transgenic mice display neurological deficits starting at around 6 weeks of age and have a severely shortened life span. We describe that MeCP2-Tg mice display selective neurodegeneration in the brain, affecting cortical neurons, hippocampal neurons, and Purkinje neurons of the cerebellum. Neuronal loss in the cortex and hippocampus is preceded by an upregulation of glial fibrillary acidic protein (GFAP) and of the microtubule-associated protein, Tau. It is noteworthy that increased expression of GFAP and Tau have both been found to be sufficient to promote neurodegeneration in *Drosophila* and mice [15–18]. Results from cell culture experiments utilizing cultured MeCP2-Tg neurons and astrocytes indicate that neurodegeneration in MeCP2-Tg mice results from a disruption of glutamate homeostasis in astrocytes. This leads to an increase of Tau in neurons and their death by excitotoxicity.

Methods

Mice

MeCP2-Tg3 mice were purchased from Jackson Laboratories (Bar Harbor, ME; stock number 008680, https://www.jax.org/strain/008680). Mice were housed in a temperature-, humidity-, and light-controlled room (12-h light/dark cycle, lights on 6:00 AM-6:00 PM). Food and water were available ad libitum. All procedures were conducted in accordance with the National Institutes of Health Guide for the Care and Use of Laboratory Animals as approved by the Southern Methodist University Institutional Animal Care and Use Committee (IACUC). Unless otherwise noted, all mice used in this study were male.

Genotyping

Genotyping of MeCP2-Tg mice was performed as previously described [19, 20]. Briefly, DNAwas extracted from mouse toe-clips using the REDExtract-N-Amp Tissue PCR Kit from Sigma-Aldrich (St. Louis, MO), and the DNA obtained was used in PCRs to determine genotype (MeCP2 transgene forward - 5'-CGCTCCGCCCTATCTCTGA-3', MeCP2 transgene reverse - 5'-ACAGATCGGATAGAAGACTC-3'; MeCP2 internal positive control forward - 5'-CAAATGTTGCTTGT CTGGTG-3', MeCP2 internal positive control reverse - 5'- GTCAGTCGAGTGCACAGTTT-3').

Behavior

Open Field

Open-field locomotor testing was conducted using the Truscan system from Coulbourn Instruments (Whitehall, PA) as previously described [21].

Grip Strength

The grip strength meter, purchased from San Diego Instruments (San Diego, CA), was used to assess neuro-muscular functional differences by recording the peak force each mouse exerted by grasping a grip bar placed at the mouse's forelimbs or hindlimbs. For this test, mice were acclimated to the room for 15 min prior to testing, and then mice were allowed to grasp a grip bar and gently pulled backwards along a horizontal plane. Tension (grip strength (GS)) applied to the grip during the trial was recorded until the mouse lost its grip. Tests were repeated three consecutive times with the maximum peak tension recorded during each trial. Trials were then averaged for analysis.

ROTOR-ROD

For training, animals were allowed to habituate to the testing room for 30 min in their home cages. Following a 5 min habituation to the stationary rod, the training program began with a speed of 5 r.p.m. In the event of a fall, subjects were placed back onto the rod until they had remained for a total of 300 sec. This training protocol was repeated for a total of three sessions with a 5 min break between each session. Training was repeated for three consecutive days. For testing, animals were habituated to the testing room as previously described. The testing program began at 0 r.p.m., increasing to 40 r.p.m. incrementally over 300 sec. Latency to fall was measured for each subject and recorded in ROTOR-ROD software (SD Instruments) and repeated for three trials with a5 min break between each trial.

Y-maze

Mice were allowed to habituate to the testing room for 30 min. After habituation, each mouse was then allowed to explore the A and B arms of the Y-maze for 15 min with the novel C arm blocked from exploration. After exploration, the Y-maze was cleaned and each mouse was then allowed to explore the A, B, and C arms of the Y-maze for 5 min while being video recorded. After testing, videos were scored for the number of entries into each arm, and then data was expressed as a percentage of entries into each arm during this 5 min time period.

Novel Object

Mice were allowed to habituate to the testing room for 30 min. Following habituation, each mouse was placed in an open chamber with two identical objects and allowed to explore freely. After 10 min, the mouse was removed and the chamber and objects were cleaned. The mouse was then placed back in the chamber with one of the original objects and one new object and allowed to freely explore for 5 min while being video recorded. After testing, videos were scored for time spent exploring each object, and the data expressed as a ratio of the time spent exploring the novel object to the time spent exploring the familiar object. Object placement was randomized in order to mitigate potential place preference.

Western Blot

Western blot analysis was conducted as previously described [21]. PVDF membranes were probed with the following antibodies: anti-MeCP2 (Cell Signaling, Beverly, MA; 1:1000, catalog number 3456S), anti-total Erk (Cell Signaling, 1:1000, catalog number 9102L), anti-NeuN (Cell Signaling, 1:1000, catalog number D4640), anti-GFAP (Cell Signaling, 1:1000, catalog number 3670), anti-Iba1 (Wako, Osaka, Japan; 1:500, catalog number 019–19741), anti-glutamine synthetase (Millipore, Billerica, MA; 1:1000, catalog number MAB302), anti-Glast (EAAT1) antibody (Abcam, Cambridge, MA; 1:1000, catalog number ab416), anti-MAP2 (Sigma-Aldrich, St. Louis, MO; 1:500, M4403), anti-Tau46 (Cell Signaling, 1:1000, catalog number 4019), anti-α-tubulin (Sigma-Aldrich, 1:40000, catalog number T5168), anti-Tau RD4 (Millipore, 1:1000, catalog number 05–804), anti- pTau262 (Santa Cruz Biotechnology, Dallas, TX; 1:1000, catalog number sc-101813), and anti-pTau404 (Santa Cruz Biotechnology, 1:1000, catalog number sc-12952-R). The Glt1 antibody was a kind gift from Jeffrey Rothstein.

Histology

Histology and histological analysis were conducted as previously described [21]. DAB staining was conducted using the Vectastain Elite ABC Kit (Burlingame, CA) following manufacturer's instructions. TUNEL staining was conducted using the TUNEL Kit from Promega (Madison, WI; catalog number G3250) following manufacturer's instructions. The following antibodies were used in histology: NeuN (Cell Signaling, 1:300, catalog number D4640), NeuN (Millipore, 1:300, catalog number MAB377), SATB2 (Abcam, 1:500, catalog number ab51502), CTIP2 (Abcam, 1:500, catalog number ab18465), Calbindin (Sigma-Aldrich, 1:400, catalog number C2724), GFAP (Dako, Carpinteria, CA, 1:500, catalog number Z0334), and Iba1 (Wako, 1:500, catalog number 019–19741).

RT-PCR

RT-PCR analysis was performed as previously described [22].

The primers used for PCR amplification are as follows:

GFAP forward 5'-GAGCGTGCAGAGATGATGGA-3'

GFAP reverse 5'-TCTCCTCCTCCAGCGATTCA-3'

Tau 4R and 3R primers:

Mouse exon 1F 58–5’-TCCGCTGTCCTCTTCTGTC-3’

Mouse exon 5R 58–5’-TTCTCGTCATTTCCTGTCC-3’

Tau 0N, 1N, and 2N primers:

Mouse exon 9R 58–5’-CACCAAAATCCGGAGAACG-3’

Mouse exon 11R 58–5’-CTTTGCTCAGGTCC ACCCGGC-3’

Isolation and Culture of Astrocytes From Mouse Cortex

Astrocyte cultures were prepared from postnatal day 1 mouse pups. Prior to dissection, astrocyte culture media (DMEM, high glucose + 10% heat-inactivated fetal bovine serum + 1% penicillin/streptomycin) was prewarmed. The mouse brain was removed and placed in a dish of HBSS; the cortices were carefully dissected; and then, the meninges from the cortex hemispheres were removed by pulling with forceps. Each cortex was cut into small pieces and placed into a tube with HBSS and 2.5% trypsin. The cortical tissue was then incubated in a 37 °C water bath for 12 min and was gently agitated every 2 min. After incubation, the tissue was centrifuged at 3000×*g* for 5 min. The supernatant was decanted and tissue was dissociated through pipetting in astrocyte culture media. After plating, the astrocyte culture media was changed every 2 days, and at 7 days, the astrocytes were split. Once the purity of the culture was determined through immunocytochemistry, the astrocytes were used for experiments.

Cortical Neuron Culture, Conditioned Media Treatment, and Live/Dead Assay

Cortical cultures were prepared from embryonic day 17–18 rat pups as previously described [22, 23]. For generation of pure neuronal cultures, 18 h after plating, 1 μM Ara-C (cytosine arabinoside) was added to the wells to prevent the proliferation of glial cells. For generation of mixed neuronal cultures, the dissociated cells were plated in media containing 10% FBS to encourage the proliferation of glial cells. On day 5, 300 μl of media was removed from each well of cortical neurons in a 24-well plate and 400 μl of conditioned media was added. For MK-801 treatment, each well was pretreated for 20 min with MK801 and then conditioned media was added. After incubating neurons in conditioned media for 48 hr, neuronal viability was determined using the Live/Dead Cytotoxicity Kit (Invitrogen; Carlsbad, CA) according to manufacturer’s instructions.

Experimental Design and Statistical Analysis

All cell culture and biochemical experiments were performed at least three times. For viability measurements, each experiment was performed in duplicate and repeated at least thrice. All *in vivo* experiments, including behavioral analyses, were performed using a minimum of six mice per condition and genotype. All statistical analyses were done using GraphPad Prism software. Data was analyzed by an unpaired Student’s t- test (Figs. 1, 2, 3, 4, 5, 6, 7, 8, 9, and 11) or two-way ANOVA (Newman-Kuels post hoc test) for Fig. 10a, b. Data are expressed as the mean ± S.D. *, **, or *** denotes a p value of <0.05, <0.01, or < 0.001, respectively.

Results

MeCP2-Tg Mice Recapitulate the Neurological and Non-Neurological Abnormalities of MeCP2 Triplication Syndrome

Although variability between mice is observed, male MeCP2-Tgmice express MeCP2 at levels that are 3.3 times higher that their wild-type littermates (Fig. 1a–c). This is consistent with information provided by Jackson Labs, which indicates that the transgene is expressed at three to five times the normal level (https://www.jax.org/strain/008680). An initial characterization of MeCP2-Tg mice has been previously reported [14]. Hypotonia, seizures, anxiety, and social behavior deficits, commonly seen in patients with *MECP2* duplication/triplication syndrome, were described in that study [14]. We have extended the characterization. As observed in patients, male MeCP2-Tg mice appear normal at birth but display neurological abnormalities subsequently. Forepaw clasping is observed by 6 weeks of age (Fig. 2a) as is reduced hindlimb strength (Fig. 2b). No reduction is seen in forelimb strength, however (Fig. 2c). Reduced motor ability at 6 weeks is confirmed using the ROTOR-ROD assay (Fig. 2d). Open-field locomotor tests reveal normal locomotion at 6 weeks but reduction at 9 weeks (Fig. 2e). Cognitive impairment was also revealed in Y-maze tests (Fig. 2f) and in the novel object recognition test (Fig. 2g). Ataxia and obvious movement deficits are observed at around 15 weeks. The neurological deficits are progressive and the mice die at 18–20 weeks. Macrocephaly has been reported in patients with *MECP2* trip-lication syndrome. MeCP2-Tg mice also display reduction in body weight, increase in brain weight, and increase in body to brain weight ratio (Fig. 2h–j). Life span, brain weight, body weight, and behavioral performance are normal in female MeCP2-Tg mice (Supplemental Fig. 1). We have found that, like patients [24], MeCP2-Tg mice display signs of constipation (data not shown). Taken together, our results along with those described previously [14] demonstrate that MeCP2-Tg mice faithfully recapitulate the major abnormalities of *MECP2* triplication syndrome.

Delayed Neuronal Loss in MeCP2-Tg Mice

We performed im- munohistochemistry with two different antibodies against NeuN. No difference in the pattern of staining or number of NeuN-positive cells between MeCP2-Tg mice and wild-type littermates is observed in the cortex, hippocampus, striatum, or cerebellum, at 10 weeks of age (Fig. 3). At 12 weeks, however, a slight reduction in the number of NeuN-positive cells is detectable in the cortex, and by 15 weeks, a 29.3% reduction is observed in the somatomotor region of the cortex (Fig. 4a, c, d) and a 24.4% reduction in the CA1 region of the hippocampus (Fig. 4b–d). Results showing reduced NeuN-positive cell numbers in the cortex and hippocampus obtained using fluorescence-based immunohistochemistry were confirmed using 3,3’-diaminobenzidine (DAB) staining (Fig. 4e). Western blots further confirmed that NeuN levels in the whole cortex and hippocampus are normal at 10 weeks but are reduced at 15 weeks (Fig. 3e and 4f, respectively). We did not observe a significant change in NeuN-positive cell numbers or level of NeuN expression in the cerebellum (Fig. 3d, e, respectively). Expression of a neuron-specific form of β-tu- bulin, β-III tubulin, is also reduced in the cortex and hippo-campus of MeCP2-Tg mice confirming that loss of neurons, rather than a reduction of NeuN or β-III tubulin expression, is responsible for the reduction in immunostaining (not shown).

We extended our analyses using antibodies to CTIP2 and SATB2, two transcription factors that are expressed in specific cell populations in the developing and mature brain [25]. In the mature cortex, CTIP2 stains deep-layer projection neurons, whereas SATB2 stains superficial layers preferentially. While SATB2-positive neurons in layers II and III of the somatomotor cortex are reduced by 21.4% in MeCP2-Tg mice at 15 weeks, CTIP2-positive neurons in layers V and VI are reduced by only 6.13%, suggesting that upper layer neurons are selectively lost in the transgenic brain (Fig. 4a, b). Within the CA1 region of the hippocampus, there is a loss of 13.9% of CTIP2-positive neurons (Fig. 5b). No cell loss is discernible in the striatum and other neuronal populations of the hippocampus at 15 weeks, suggesting selectivity in vulnerability to elevated MeCP2 (Fig. 4c, d). In the cerebellum, the molecular and internal granule layer appears normal. However, there is obvious loss of Purkinje neurons, which is more noticeable in the posterior lobes, particularly lobe VII (Fig. 5c). Regional differences in neurodegeneration within the cerebellum have been noted in various spontaneous mouse mutants, including the leaner and tottering mutants, as well as genetically engineered mouse mutants [26].

Selective cell loss in the upper cortical layers and hippo-campus was confirmed at 15 weeks using DAPI staining to detect pyknotic nuclei and TUNEL staining to detect apoptotic cells (Fig. 6a, b). Consistent with the results using NeuN staining, we do not detect TUNEL-positive cells in the striatum (data not shown). As ascertained from NeuN immunohis-tochemistry, there is no increase in pyknotic nuclei or TUNEL staining in MeCP2-Tg cortex at 10 weeks (data not shown), confirming that neuronal loss occurs at some point after 10 weeks of age.

Selective Upregulation of GFAP Expression in MeCP2-Tg Mice

We used GFAP immunostaining to evaluate the status of astrocytes in the MeCP2 brain. Interestingly, at 15 weeks of age, MeCP2-Tg mice consistently display a robust increase in GFAP staining and GFAP staining intensity in the cortex and hippocampus (Fig. 7a). While the increase in GFAP staining is not generally observed in the cerebellum, in a few mice that displayed a severe phenotype and high GFAP upregula- tion in the cortex and hippocampus, some increase is observed even in the cerebellum at 15 weeks (data not shown). Interestingly, we have noted an increase in GFAP limited to lobe 7 of the cerebellum (data not shown). Other brain regions showed no increase in GFAP staining. Two aspects of the increased GFAP staining in the somatomotor cortex are interesting: (1) the increase in staining is variable and (2) while all MeCP2-Tg mice displayed increased GFAP staining, many had staining only in the outer half (pial half) or outer third or high aggregations of staining in this area of the cortex beginning around 10 weeks of age (Fig. 7a, e). Thus, the pattern of elevated GFAP staining correlates with the location of where most neuronal loss is observed. Increased GFAP expression was confirmed by Western blot analysis (Fig. 7b). RT-PCR analysis also revealed elevated GFAP messenger RNA (mRNA), suggesting that this is transcriptionally mediated (Fig. 7c). GFAP immunostaining is often used to evaluate neuroinflammation that typically occurs after neuronal loss. In models of neurodegenerative disease as well as in the brains of patients, astrocyte activation and gliosis is a response to the degeneration of neurons and is limited to the area surrounding the dying neurons [27]. As described above and shown in Fig. 7a, increased GFAP staining is concentrated in the

upper layers and can extend down through the lower layers of the MeCP2-Tg cortex. More interestingly, the increase in GFAP staining is observed in the MeCP2 cortex and hippocampus even at 10 weeks, when neuronal loss is not detectable (Fig. 7e). Western blot analysis shows a slight increase in GFAP expression in the cortex and hippocampus of 10-week-old MeCP2-Tg mice (Fig. 7d). The upregula- tion of GFAP before the commencement of neuronal loss argues against it being part of a neuroinflammatory response, which generally results from neurodegeneration. No increase in GFAP expression is observed in the MeCP2-Tg cortex or hippocampus of MeCP2-Tg mice at 3 weeks (data not shown).

Staining with Iba-1, a marker for microglia, reveals no increase in Iba1-positive cell numbers or expression in the MeCP2-Tg cortex at 15 weeks confirming the lack of a neuroinflammatory response (Fig. 8a, b). Furthermore, the morphology of Iba1-positive cells in the MeCP2-Tg cortex is not different from those in the wild-type cortex, indicating that they are not activated (Fig. 7a). Levels of glutamine synthase or GLT-1 transporter are also unchanged in MeCP2-Tg mice, indicating that the GFAP increase is not due to astrogliosis (Fig. 8c, d). In contrast, the expression of GLAST/EAAT1 glutamate transporter is reduced in MeCP2- Tg mice (Fig. 8e). Reduced GLAST1 expression has been shown to cause seizures in mice and humans and explains the seizures observed in patients with MeCP2 triplication syndrome [28, 29].

GFAP Is Upregulated in the Spinal Cord Earlier Than in the Brain

The motor impairment detected by grip strength and rotorod assays at 6 weeks led us to examine whether abnormalities in the spinal cord precede those in the brain. Indeed, examination of the spinal cord shows increased GFAP staining even at 6 weeks (Fig. 9a). The increase was more pronounced in the lumbar portion compared with the cervical portion of the spinal cord, consistent with hindlimbs being selectively affected at 6 weeks. Interestingly, we did detect a decrease in NeuN+ cells in the dorsal horn and an increase in active-caspase-3 staining revealing cell death in the dorsal horn at 6 weeks (Fig. 9b, c). These results suggest that neurological impairment at 6 weeks could be due to degeneration in the spinal cord. Analyses of the spinal cord of MeCP2-Tg mice at 3 weeks revealed no increase in GFAP, suggesting that the increase occurred between 3 and 6 weeks (data not shown). Similarly, no motor impairment was discernible at 3 weeks (data not shown).

Selective Upregulation of Tau Expression in MeCP2-Tg Mice

MeCP2 regulates microtubule structure and dynamics both in astrocytes and neurons [30, 31]. We examined the expression of the microtubule-associated protein MAP2, which is localized mainly in dendrites, and Tau, which is present mainly in axons. Expression of MAP2a and MAP2b is unaltered in the MeCP2-Tg brain (Fig. 10a). However, Tau expression is significantly increased in the cortex, hippocampus, and to a lesser degree, the cerebellum of MeCP2-Tg mice (Fig. 10b). Furthermore, the ON4R and 2N4R isoforms of Tau increase significantly in the cortex and hippocampus (Fig. 10c). The extent of increase varied, as described above for GFAP staining. As observed with total Tau, levels of Tau phosphorylated at Ser262 (Fig. 10d) and Ser404 (not shown) increased. However, when p-Tau is expressed as a ratio of Tau, there is no significant change in Tau phosphorylation at Ser262 (Fig. 10d) or Ser404 (not shown). In contrast to the elevation in GFAP mRNA, Tau

mRNA is not increased in MeCP2-Tg brain (Fig. 10e), suggesting that the increase in Tau protein is mediated posttranscriptionally and likely to be due to enhanced protein stability.

Astrocytes Trigger Excitotoxic Death in MeCP2-Tg Mice

The finding that increased expression of GFAP precedes the up- regulation of Tau and neurodegeneration in the cortex of MeCP2-Tg mice suggests that astrocytic dysfunction could trigger disease pathogenesis in the brain, possibly through the release of a neurotoxic factor. Contribution of an astrocyte-released neurotoxic factor has been implicated in the pathogenesis of several neurodegenerative diseases. To investigate the possibility that an astrocyte-derived factor contributes to neuronal death in the MeCP2-Tg brain, we expressed MeCP2 (both isoforms, E1 and E2, individually and in combination) in primary astrocytes cultured from the cortex of wild-type mice. We exposed wild-type cortical neurons to conditioned medium from these MeCP2-overexpressing astrocytes, henceforth referred to as MeCP2- ACM. While MeCP2-ACM from both E1 and E2 overex-pressing astrocytes was toxic, expressing both isoforms (E1 + E2) showed highest toxicity with over 50% of the neurons dying after 48 h (Fig. 11a). As observed with normal astrocytes overexpressing MeCP2, ACM from astrocytes cultured from MeCP2-Tg mice was also toxic to wild- type cortical neurons (Fig. 11b). We next transduced astrocytes cultured from the cerebellum with MeCP2. MeCP2-ACM from cerebellar astrocytes displayed no toxicity when added to cortical neurons (not shown). Similarly, MeCP2-ACM from the U251 astrocyte cell line (not shown) had no effect on the viability of cortical neurons. These findings indicate that the neurotoxic factor was produced selectively by cortical astrocytes.

Heat inactivation and freeze-thawing of cortical MeCP2- ACM had no effect on its neurotoxic effect (data not shown), suggesting that the neurotoxic factor >was not a protein. We explored the possibility that the factor was glutamate, which at elevated levels would cause excitotoxicity via overstimulation of NMDA/AMPA receptors. Consistent with excitotoxicity, the NMDAR antagonist, MK-801 (blocks pore of NMDAR), inhibits neurotoxicity by MeCP2-ACM (Fig. 11a). Toxicity by ACM from cortical neurons cultured from MeCP2-Tg mice was also blocked by MK-801 (Fig. 11b).

Analysis of GFP-ACM and MeCP2 ACM from neuronal, astrocytic, and mixed cultures revealed that the increase in extracellular glutamate concentration was dependent on the presence of astrocytes (Fig. 11c).

Chronic excitotoxicity is an important contributor in slow-progressing neurodegenerative diseases, including Alzheimer’s disease, Huntington’s disease, and ALS. Interestingly, studies by other labs have found that Tau expression is increased by excitotoxicity, suggesting that the elevation in Tau in the MeCP2-Tg brain may be due to excitotoxicity induced by astrocyte dysfunction [32–34]. However, treatment of cortical neurons with ACM from astrocytes overexpressing MeCP2 or from male MeCP2-Tg mice induced Tau only slightly, suggesting that cell autonomous changes in neurons resulting from extended elevation of MeCP2 is the major contributor to increased Tau (Fig. 11d, e).

Female MeCP2-Tg Mice Express Elevated MeCP2 but Display Normal GFAP and Tau Expression

In humans, females with *MECP2* triplication syndrome suffer mild psychiatric symptoms or are asymptomatic. This is believed to be due to heavily skewed inactivation of the abnormal X-chromosome permitting expression predominantly from the single normal X chromosome. We find that female transgenic mice express MeCP2 at about two times higher than normal (1.94-fold) (Fig. 12a), whereas male MeCP2-Tg expression was about three times higher (3.3-fold) (Fig. 1c). However, the approximately 2-fold higher expression of MeCP2 in females suggests that, at least in mice, skewing of the defective chromo-some is inefficient. We verified that the human transgene was efficiently expressed in female MeCP2-Tg mice by RT-PCR (Fig. 12b). Despite expressing about twice the level of MeCP2, ACM from the cortex of female MeCP2-Tg mice did not contain elevated glutamate and was not toxic to cortical neurons (Fig. 12c–e). Moreover, the increased GFAP and reduced GLAST displayed by male MeCP2-Tg astrocytes was not observed in female MeCP2-Tg astrocytes (Fig. 12f). This suggests that for elevation of GFAP and disruption of glutamate homeostasis in astrocytes, expression of MeCP2 has to cross a certain threshold, which is not reached in female MeCP2-Tg astrocytes. To test this, we overexpressed MeCP2 in normal (WT) male and female astrocytes. We found that ACM from both WT male and female astrocytes overexpressing MeCP2 was toxic to cortical neurons (data not shown). In MeCP2 Tg mice, when we compared the increase in Tau expression to the fold change in MeCP2 levels, we found a correlation in MeCP2-Tg male mice ($r^2 = 0.8$) but not in MeCP2-Tg female mice (Supplemental Fig. 2). Taken together, these results suggest regulation of GFAP and Tau expression, and by extension, the gender-specific neurological abnormalities in MeCP2-Tg mice requires highly elevated MeCP2 which is not attained in female mice and cells because of expression from the normal X chromosome.

Discussion

We report that male MeCP2-Tg mice display macrocephaly and progressive neurological deficits, including motor and cognitive deficits, ataxia, and a severely shortened life span. These are abnormalities also seen in patients with *MECP2* duplication and triplication syndrome. Seizures, another common issue in patients, have previously been described in MeCP2-Tg mice [14]. We find that hindlimbs are selectively weakened in MeCP2-Tg mice. Greater effect on lower limb strength has also been described in *MECP2* triplication syndrome patients [8]. As in patients, some variability in symptom severity and non-neuronal abnormalities, such as constipation, are also observed in MeCP2-Tg mice. Female MeCP2-Tg mice do not display discernible neurological deficits, recapitulating the situation in humans where females are asymptomatic or mildly affected.

Although we have observed abnormalities in the spinal cord of MeCP2-Tg mice even at 6 weeks of age that likely contribute to motor impairment, in this study we have focused on the brain. MeCP2-Tg mice display neuronal loss in the cortex and hippocampus. Within the cortex, upper layers are more affected, while within the hippocampus, the CA1 region is most affected. Within the cerebellum, Purkinje neurons suffer degeneration but granule neurons are unaffected. These results indicate selectivity in vulnerability to elevated MeCP2.

Although confirmation will depend on careful analysis of patient tissue, which is currently unavailable, based on the neuronal death in MeCP2-Tg mouse brain we propose that MeCP2 duplication/triplication syndrome is a neurodegener- ative disorder. Our conclusion is supported by MRI studies describing cortical atrophy in patients with *MECP2* duplication syndrome [9,11,12]. Diffuse loss of neurons in the cortex and extensive loss of Purkinje neurons has also been reported [13, 35–37].

A recent study described abnormal dendritic arborization and spine morphology in MeCP2 transgenic mice, but no cell loss [38]. However, analyses of cell numbers in this study were done on 9-week-old mice an age at which there is no neuronal death even in our analyses. Another major difference between our study and the one by Jiang et al. was that in their study the MeCP2-Tg1 line was used. This line expresses MeCP2 at about two times the normal level and displays symptoms that are relatively mild compared to patients with MeCP2 duplication/triplication syndrome [14]. In our analyses of MeCP2-Tg3 line, we found that MeCP2 protein is expressed at 3.3 times the normal level, which agrees with the 3–5-fold higher expression that Jackson Labs reports in their data sheet for this transgenic line. Thus, these mice express MeCP2 at a level that is slightly higher than MeCP2 triplication disorder patients. As observed in a variety of other mouse genetic models of neurodevelopmental and neurodegenerative disorders, mimicking of human abnormalities in mice often requires a higher level of mutant gene expression than in patients. Although it would be interesting to analyze other models of *MECP2* duplication/triplication syndrome, like the Tg-1 line, in which MeCP2 is expressed at patient levels, the failure of such mouse models to recapitulate key features and the severity of the human disorders suggests that molecular and cellular alterations responsible for the neurological abnormalities do not occur in these mouse models. Whether analyses of these mouse models will provide a substantive understanding of disease mechanisms is therefore debatable.

MeCP2-Tg mice display highly elevated expression of GFAP in the hippocampus and cortex. In a few older mice displaying more severe neurological deficits, a small increase in GFAP is observed in the cerebellum also. This suggests that while the cortex and hippocampus are most vulnerable, the increase in GFAP could occur in other brain parts at late stages of the disorder. In fact, results of three separate microarray analyses by the Zoghbi lab using amygdala, cerebellum, and hippocampus from MeCP2-Tg mice revealed that GFAP mRNA upregulation occurs in all three brain parts, although this finding was not noted or pursued further [39–41]. While increased GFAP is generally regarded as a marker of neuroinflammation, it can occur independently of a neuroinflammatory response and by itself cause neurological deficits. This occurs in Alexander disease (AxD), an astrogliopathy caused by mutations in GFAP resulting in its accumulation in astrocytes of the hippocampus and cortex [42, 43]. Patients with type-1 AxD display macrocephaly, seizures, developmental retardation, hypoactivity, and shortened life span. While the primary cause is astrocyte dysfunction, type-1-AxD patients display variable neuronal loss in the hippocampus, cortex, and striatum [18, 43, 44]. The neurological abnormalities and early death of AxD can be recapitulated in mice and flies by overexpression not only of mutant forms of GFAP but also of normal GFAP [18, 45–47]. In AxD, a reduction in the level of the GLT1 glutamate transporter in vulnerable brain regions has been suggested to affect glutamate clearance leading to excitotoxic death of neurons [48–50]. Similarly, in MeCP2-

Tg mice, the increased expression of GFAP and reduction in GLAST is most pronounced in the MeCP2-Tg cortex and hippocampus, where neuronal loss occurs subsequently. Our results suggest that rather than being a disorder that is primarily neuronal in nature, the trigger for disease pathogenesis in *MECP2* triplication disorder is astroglial dysfunction. If so, *MECP2* triplication disorder would join a growing list of neurodevelopmental and neurodegenerative disorders in which glia play an essential role in disease pathogenesis [51, 52].

Another novel observation is the increased expression of Tau in the MeCP2-Tg brain. In both *Drosophila* and mice, overexpression of Tau in the CNS results in progressive neurodegeneration [15, 16, 32, 34, 53]. Interestingly, expression of Tau mRNA is not elevated, indicating that the increase in protein occurs by a posttranscriptional mechanism. Consistently, Tau mRNA was not identified as differentially expressed in any of the microarray gene expression studies conducted by the Zoghbi lab [39–41]. Although our analysis of two sites, Ser 262 and Ser404, revealed no increase in the extent of Tau phosphorylation in MeCP2-Tg mice, it is possible that phosphorylation is elevated at other residues.

As observed *in vivo*, GFAP is elevated in astrocytes cultured from the cortex of MeCP2-Tg mice and even in normal cortical astrocytes in which MeCP2 is overexpressed. Furthermore, CM from these astrocytes induces death of normal cortical neurons. In contrast, CM from cerebellar astrocytes is not toxic to cortical neurons, suggesting that cortical astrocytes are more vulnerable to elevated MeCP2. Neurotoxicity from cortical MeCP2-Tg astrocyte CM is accompanied by Tau upregulation. The abrogation of CM- mediated neurotoxicity by MK-801, which also inhibits the increase in Tau expression, suggests that both Tau induction and neuronal death are due to NMDA receptor-mediated excitotoxicity. Previous studies have found that upregulation of Tau following excitotoxic insult can be blocked by MK801 and other NMDA receptor antagonists [54–57]. Furthermore, lowering Tau levels can protect against excitotoxicity, suggesting that excitotoxic neuronal loss requires Tau upregulation [58, 59]. Accumulating evidence suggests that reducing Tau also can reduce seizures and protect against neurological and cognitive deficits in multiple mouse models of Alzheimer's disease (AD) and traumatic brain injury [60–64]. Unlike CM from male MeCP2-Tg astrocytes, CM from female astrocytes does not induce Tau in neurons and is not neurotoxic. Although this could be because of highly skewed X-chromosome inactivation of the chromosome with the transgene, we were surprised to find that the MeCP2 transgene is efficiently expressed in the cortex of female MeCP2-Tg mice. While lower than in male MeCP2-Tg mice, Western blot analysis revealed that the total level of MeCP2 in the female MeCP2-Tg cortex is almost 2-fold higher than normal. Although further analyses is needed, our finding that female MeCP2-Tg mice express the transgene efficiently and produce elevated MeCP2 argues against the general belief that women with MeCP2 duplication or triplication on the X chromosome are largely asymptomatic because of highly skewed X-chromosome inactivation. A likely explanation is that in both humans and in mice, MeCP2 expression has to cross a certain threshold before pathological mechanisms are triggered. Because females with *MECP2* gene duplication also express MeCP2 from the normal X chromosome, the total level of MeCP2 is lower than in males and thus lower than the pathological threshold. In the MeCP2-Tg mice, the threshold is likely to be ~3-fold higher

than normal, which is crossed in male MeCP2-Tg mice, but not female mice. This may also explain why even male mice of the TG-1 line of Collins et al. [14, 38], which have an ~2-fold elevation in MeCP2, do not display the severe phenotype observed in MeCP2-Tg mice (TG-3 line) and patients. Indeed, in preliminary experiments, we find that when MeCP2 is overexpressed in normal female cortical astrocytes (at levels that are several fold higher than normal), high levels of glutamate are present in the ACM and the ACM is toxic to neurons (data not shown). Also conceivable however, and not mutually exclusive with the threshold hypothesis, is that female astrocytes (and perhaps neurons) may have protective mechanisms capable of preventing astrocyte dysfunction and excitoxicity. One candidate for such protection could be estrogens.

In summary, we propose for the first time that *MECP2* triplication syndrome is a neurodegenerative disorder. The severe cognitive impairment and ataxia suffered by patients with *MECP2* duplication and triplication syndrome is consistent with neuronal loss in the cortex, hippocampus, and cerebellum. We suggest that astrocytic dysfunction resulting from an upregulation of GFAP leads to defective glutamate homeostasis, which through excitoxicity and an elevation of Tau levels kills neurons (Fig. 13). Reduction of Tau has been shown to reduce seizures, excitotoxicity, and neurodegeneration. Pharmacological agents, anti-sense oligonucleotides, or CRISPR-mediated approaches targeting Tau or GFAP may represent an attractive therapeutic approach for *MECP2* duplication/triplication syndrome. Blocking excitotoxicity by inhibition of NMDA receptors could be another effective approach to treat this devastating disorder.

Supplementary Material

Refer to Web version on PubMed Central for supplementary material.

Acknowledgements

This research was supported by a grant from the National Institutes of Health (R01 NS040408). We thank Dr. Jade Franklin for making significant contributions to the research and the preparation of figures for the manuscript. We also acknowledge the contribution of Dr. Xiaoju Zou for her assistance with some of the immunohistology work described in the manuscript.

References

1. Adkins NL, Georgel PT (2011) MeCP2: Structure and function. Biochem Cell Biol (Can) 89:1-11
2. Guy J, Cheval H, Selfridge J, Bird A (2011) The role of MeCP2 in the brain. Annu Rev Cell Dev Biol (U S) 27:631-652
3. Hite KC, Adams VH, Hansen JC (2009) Recent advances in MeCP2 structure and function. Biochem Cell Biol (Can) 87:219-227
4. Ausio J, Martinez de Paz A, Esteller M (2014) MeCP2: The long trip from a chromatin protein to neurological disorders. Trends Mol Med (Engl) 20:487-498
5. Chahrour M, Zoghbi HY (2007) The story of rett syndrome: From clinic to neurobiology. Neuron (U S) 56:422-437
6. Lombardi LM, Baker SA, Zoghbi HY (2015) MECP2 disorders: From the clinic to mice and back. J Clin Invest (U S) 125: 2914-2923
7. Peters SU, Hundley RJ, Wilson AK, Carvalho CM, Lupski JR, Ramocki MB (2013) Brief report: Regression timing and associated features in MECP2 duplication syndrome. J Autism Dev Disord 43: 2484-2490 [PubMed: 23456562]

8. Ramocki MB, Tavyev YJ, Peters SU (2010) The MECP2 duplication syndrome. Am JMedGenetA (U S) 152A:1079-1088

9. Van Esch H (2012) MECP2 duplication syndrome. Mol Syndromol 2:128-136 [PubMed: 22679399]

10. Tang B, Becanovic K, Desplats PA, Spencer B, Hill AM, Connolly C, Masliah E, Leavitt BR et al. (2012a) Forkhead box protein p1 is a transcriptional repressor of immune signaling in the CNS: Implications for transcriptional dysregulation in Huntington disease. Hum Mol Genet (Engl) 21:3097-3111

11. Lugtenberg D, Kleefstra T, Oudakker AR, Nillesen WM, Yntema HG, Tzschach A, Raynaud M, Rating D et al. (2009) Structural variation in Xq28: MECP2 duplications in 1% of patients with unexplained XLMR and in 2% of male patients with severe encephalopathy. Eur J Hum Genet (Engl) 17:444-453

12. Shimada S, Okamoto N, Ito M, Arai Y, Momosaki K, Togawa M, Maegaki Y, Sugawara M et al. (2013) MECP2 duplication syndrome in both genders. Brain Dev (Neth) 35:411-419

13. Van Esch H, Bauters M, Ignatius J, Jansen M, Raynaud M, Hollanders K, Lugtenberg D, Bienvenu T et al. (2005) Duplication of the MECP2 region is a frequent cause of severe mental retardation and progressive neurological symptoms in males. Am J Hum Genet (U S) 77:442-453

14. Collins AL, Levenson JM, Vilaythong AP, Richman R, Armstrong DL, Noebels JL, David Sweatt J, Zoghbi HY (2004) Mild overexpression of MeCP2 causes a progressive neurological disorder in mice. Hum Mol Genet (Engl) 13:2679-2689

15. Jaworski T, Kugler S, Van Leuven F (2010) Modeling of tau- mediated synaptic and neuronal degeneration in alzheimer's disease. Int J Alzheimers Dis (Engl) 2010:1-10. 10.4061/2010/573138

16. Jaworski T, Dewachter I, Lechat B, Croes S, Termont A, Demedts D, Borghgraef P, Devijver H et al. (2009) AAV-tau mediates pyramidal neurodegeneration by cell-cycle re-entry without neurofibrillary tangle formation in wild-type mice. PLoS One (U S) 4:e7280

17. Min SW et al. (2015) Critical role of acetylation in tau-mediated neurodegeneration and cognitive deficits. Nat Med (U S) 21:1154-1162

18. Wang L, Colodner KJ, Feany MB (2011) Protein misfolding and oxidative stress promote glial-mediated neurodegeneration in an alexander disease model. J Neurosci (U S) 31:2868-2877

19. Bardai FH, Price V, Zaayman M, Wang L, D'Mello SR (2012) Histone deacetylase-1 (HDAC1) is a molecular switch between neuronal survival and death. J Biol Chem (U S) 287:35444-35453

20. Bardai FH, Verma P, Smith C, Rawat V, Wang L, D'Mello SR (2013) Disassociation of histone deacetylase-3 from normal huntingtin underlies mutant huntingtin neurotoxicity. J Neurosci (U S) 33:11833-11838

21. Norwood J, Franklin JM, Sharma D, D'Mello SR (2014) Histone deacetylase 3 is necessary for proper brain development. J Biol Chem (U S) 289:34569-34582

22. Majdzadeh N, Wang L, Morrison BE, Bassel-Duby R, Olson EN, D'Mello SR (2008) HDAC4 inhibits cell-cycle progression and protects neurons from cell death. Dev Neurobiol (U S) 68:1076-1092

23. Chen HM, Wang L, D'Mello SR (2008) A chemical compound commonly used to inhibit PKR, {8-(imidazol-4-ylmethylene)-6H-azolidino[5,4-g] benzothiazol-7-one}, protects neurons by inhibiting cyclin-dependent kinase. Eur J Neurosci (Fr) 28: 2003-2016

24. Tang SS, Fernandez D, Lazarou LP, Singh R, Fallon P (2012b) MECP2 triplication in 3 brothers - a rarely described cause of familial neurological regression in boys. Eur J Paediatr Neurol (Engl) 16:209-212

25. Molyneaux BJ, Arlotta P, Menezes JR, Macklis JD (2007) Neuronal subtype specification in the cerebral cortex. Nat Rev Neurosci (Engl) 8:427-437

26. Cerminara NL, Lang EJ, Sillitoe RV, Apps R (2015) Redefining the cerebellar cortex as an assembly of non-uniform purkinje cell microcircuits. Nat Rev Neurosci (Engl) 16:79-93

27. Maragakis NJ, Rothstein JD (2006) Mechanisms of disease: Astrocytes in neurodegenerative disease. Nat Clin Pract Neurol (Engl) 2:679-689

28. Bjornsen LP, Eid T, Holmseth S, Danbolt NC, Spencer DD, de Lanerolle NC (2007) Changes in glial glutamate transporters in human epileptogenic hippocampus: Inadequate explanation for high extracellular glutamate during seizures. Neurobiol Dis (U S) 25:319-330

29. Robel S, Sontheimer H (2016) Glia as drivers of abnormal neuronal activity. Nat Neurosci (U S) 19:28-33
30. Delépine C, Nectoux J, Bahi-Buisson N, Chelly J, Bienvenu T (2013) MeCP2 deficiency is associated with impaired microtubule stability (Germany) FEBS Lett 587:245-253
31. Nectoux J, Florian C, Delepine C, Bahi-Buisson N, Khelfaoui M, Reibel S, Chelly J, Bienvenu T (2012) Altered microtubule dynamics in Mecp2-deficient astrocytes.J Neurosci Res (U S) 90:990-998
32. Papanikolopoulou K, Skoulakis EM (2011) The power and richness of modelling tauopathies in drosophila. Mol Neurobiol (U S) 44: 122-133
33. Sun XY, Tuo QZ, Liuyang ZY, Xie AJ, Feng XL, Yan X, Qiu M, Li S et al. (2016) Extrasynaptic NMDA receptor-induced tau overexpression mediates neuronal death through suppressing survival signaling ERK phosphorylation. Cell Death Dis (Engl) 7:e2449
34. Wittmann CW, Wszolek MF, Shulman JM, Salvaterra PM, Lewis J, Hutton M, Feany MB (2001a) Tauopathy in drosophila: Neurodegeneration without neurofibrillary tangles. Science (U S) 293:711-714
35. Friez MJ, Jones JR, Clarkson K, Lubs H, Abuelo D, Bier JA, Pai S, Simensen R et al. (2006) Recurrent infections, hypotonia, and mental retardation caused by duplication of MECP2 and adjacent region in Xq28. Pediatrics (U S) 118:e1687-e1695
36. Lubs H, Abidi F, Bier JA, Abuelo D, Ouzts L, Voeller K, Fennell E, Stevenson RE et al. (1999) XLMR syndrome characterized by multiple respiratory infections, hypertelorism, severe CNS deterioration and early death localizes to distal Xq28. Am J Med Genet (U S) 85: 243-248
37. Reardon W, Donoghue V, Murphy AM, King MD, Mayne PD, Horn N, Birk Moller L (2010) Progressive cerebellar degenerative changes in the severe mental retardation syndrome caused by duplication of MECP2 and adjacent loci on Xq28. Eur J Pediatr (Germany) 169:941-949
38. Jiang M, Ash RT, Baker SA, Suter B, Ferguson A, Park J, Rudy J, Torsky SP et al. (2013) Dendritic arborization and spine dynamics are abnormal in the mouse model of MECP2 duplication syndrome. J Neurosci (U S) 33:19518-19533
39. Ben-Shachar S, Chahrour M, Thaller C, Shaw CA, Zoghbi HY (2009) Mouse models of MeCP2 disorders share gene expression changes in the cerebellum and hypothalamus. Hum Mol Genet (Engl) 18:2431-2442
40. Chahrour M, Jung SY, Shaw C, Zhou X, Wong ST, Qin J, Zoghbi HY (2008) MeCP2, a key contributor to neurological disease, activates and represses transcription. Science (U S) 320:1224-1229
41. Samaco RC, Mandel-Brehm C, McGraw CM, Shaw CA, McGill BE, Zoghbi HY (2012) Crh and Oprm1 mediate anxiety-related behavior and social approach in a mouse model of MECP2 duplication syndrome. Nat Genet (U S) 44:206-211
42. Messing A, Brenner M (2003) Alexander disease: GFAP mutations unify young and old. Lancet Neurol (Engl) 2:75
43. Messing A, Brenner M, Feany MB, Nedergaard M, Goldman JE (2012) Alexander disease. J Neurosci (U S) 32:5017-5023
44. Yoshida T, Nakagawa M (2012) Clinical aspects and pathology of alexander disease, and morphological and functional alteration of astrocytes induced by GFAP mutation. Neuropathology (Aust) 32: 440-446
45. Hagemann TL, Connor JX, Messing A (2006) Alexander disease-associated glial fibrillary acidic protein mutations in mice induce Rosenthal fiber formation and a white matter stress response. J Neurosci (U S) 26:11162-11173
46. Jany PL, Hagemann TL, Messing A (2013) GFAP expression as an indicator of disease severity in mouse models of alexander disease. ASN Neuro (Engl) 5:e00109
47. Tanaka KF, Takebayashi H, Yamazaki Y, Ono K, Naruse M, Iwasato T, Itohara S, Kato H et al. (2007) Murine model of alexander disease: Analysis of GFAP aggregate formation and its pathological significance. Glia (U S) 55:617-631
48. Minkel HR, Anwer TZ, Arps KM, Brenner M, Olsen ML (2015) Elevated GFAP induces astrocyte dysfunction in caudal brain regions: A potential mechanism for hindbrain involved symptoms in type II alexander disease. Glia (U S) 63:2285-2297

49. Sosunov AA, Guilfoyle E, Wu X, McKhann GM 2nd, Goldman JE (2013) Phenotypic conversions of “protoplasmic” to “reactive” astrocytes in alexander disease. J Neurosci (U S) 33:7439-7450
50. Tian R, Wu X, Hagemann TL, Sosunov AA, Messing A, McKhann GM, Goldman JE (2010) Alexander disease mutant glial fibrillary acidic protein compromises glutamate transport in astrocytes. J Neuropathol Exp Neurol (U S) 69:335-345
51. Ilieva H, Polymenidou M, Cleveland DW (2009) Non-cell autonomous toxicity in neurodegenerative disorders: ALS and beyond. J Cell Biol (U S) 187:761-772
52. McGann JC, Lioy DT, Mandel G (2012) Astrocytes conspire with neurons during progression of neurological disease. Curr Opin Neurobiol (Engl) 22:850-858
53. Sun M, Chen L (2015) Studying tauopathies in drosophila: A fruitful model. Exp Neurol 274:52-57 [PubMed: 25862286]
54. Boehm J (2013) A ‘danse macabre’: Tau and fyn in STEP with amyloid beta to facilitate induction of synaptic depression and excitotoxicity. Eur J Neurosci (Fr) 37:1925-1930
55. Couratier P, Lesort M, Terro F, Dussartre C, Hugon J (1996) NMDA antagonist blockade of AT8 tau immunoreactive changes in neuronal cultures. Fundam Clin Pharmacol (Engl) 10:344-349
56. Esclaire F, Lesort M, Blanchard C, Hugon J (1997) Glutamate toxicity enhances tau gene expression in neuronal cultures. J Neurosci Res (U S) 49:309-318
57. Sindou P, Couratier P, Barthe D, Hugon J (1992) A dose-dependent increase of tau immunostaining is produced by glutamate toxicity in primary neuronal cultures. Brain Res (Neth) 572:242-246
58. Pizzi M, Valerio A, Ribola M, Spano PF, Memo M (1993) A tau antisense oligonucleotide decreases neurone sensitivity to excitotoxic injury. Neuroreport (Engl) 4:823-826
59. Pizzi M, Valerio A, Arrighi V, Galli P, Belloni M, Ribola M, Alberici A, Spano P et al. (1995) Inhibition of glutamate-induced neurotoxicity by a tau antisense oligonucleotide in primary culture of rat cerebellar granule cells. Eur JNeurosci (Fr) 7:1603-1613
60. Cheng JS, Craft R, Yu GQ, Ho K, Wang X, Mohan G, Mangnitsky S, Ponnusamy R et al. (2014) Tau reduction diminishes spatial learning and memory deficits after mild repetitive traumatic brain injury in mice. PLoS One (U S) 9:e115765
61. Ke YD, Suchowerska AK, van der Hoven J, De Silva DM, Wu CW, van Eersel J, Ittner A, Ittner LM (2012) Lessons from tau-deficient mice. Int J Alzheimers Dis (U S) 2012:873270
62. Morris M, Maeda S, Vossel K, Mucke L (2011) The many faces of tau. Neuron (U S) 70:410-426
63. Roberson ED, Scearce-Levie K, Palop JJ, Yan F, Cheng IH, Wu T, Gerstein H, Yu GQ et al. (2007) Reducing endogenous tau ameliorates amyloid beta-induced deficits in an alzheimer’s disease mouse model. Science (U S) 316:750-754
64. Shipton OA, Leitz JR, Dworzak J, Acton CE, Tunbridge EM, Denk F, Dawson HN, Vitek MP et al. (2011) Tau protein is required for amyloid {beta}-induced impairment of hippocampal long-term potentiation. JNeurosci (U S) 31:1688-1692

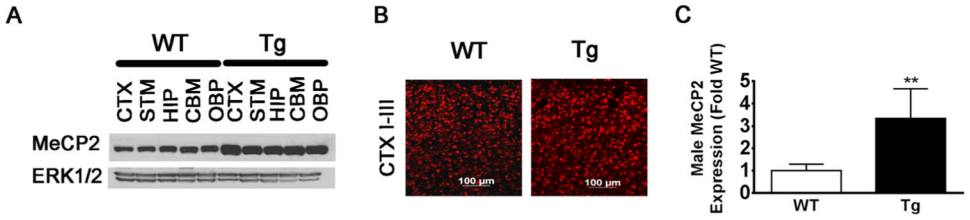

Fig. 1.

MeCP2 expression in male MeCP2-Tg mice. **a** Western blot of MeCP2 expression in different brain parts including the cortex (CTX), striatum (STM), hippocampus (HIP), cerebellum (CBM), and other brain parts (OBP) from 15-week-old MeCP2-Tg and wild-type (WT) littermate. ERK1/2 was used as a loading control. **b** MeCP2 immunohistological staining in the CTX layers I-III of 15-week-old MeCP2-Tg mice. **c** Quantification of MeCP2 protein expression from Western blot analyses of cortical lysates from 15-week-old WT and MeCP2-Tg mice. The graph represents quantification from eight pairs of WT and MeCP2-Tg mice. While each pair of WT and MeCP2-Tg mice were from the same litter, the eight pairs came from different litters of mice

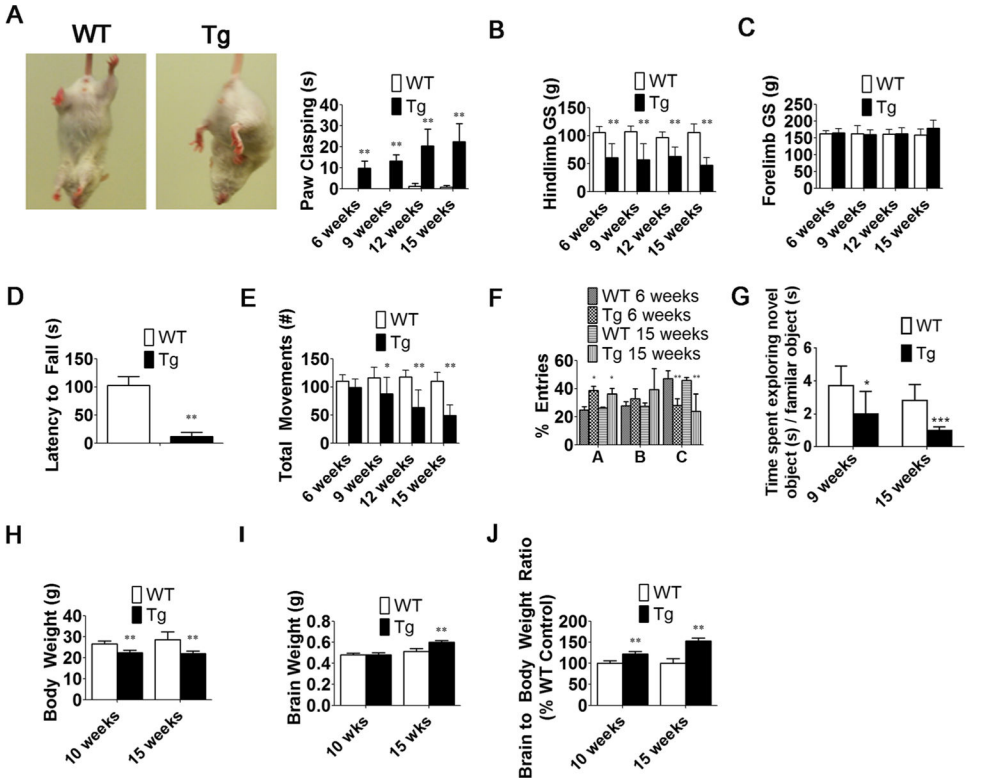

Fig. 2.

MeCP2-Tg (Tg) male mice display behavioral impairments and have increased brain weight. **a** Quantification of paw-clasping at 6, 9, 12, and 15 weeks of age (n = 9–20). **b, c** Hindlimb and forelimb grip strength at 6, 9, 12, and 15 weeks of age (n = 6) **d** Latency to fall using ROTOR-ROD. Quantification at 6 weeks (n = 6). **e** Locomotor analysis at 6, 9, 12, and 15 weeks of age (n = 9–32). **f** Y-maze entries at 6 and 15 weeks of age (n = 6). **g** Novel Object Recognition Test at 9 and 15 weeks (n = 6). **h, i** Body weight and brain weight measurements at 10 and 15 weeks (n = 12–32). j Brain to body weight ratios at 10 and 15 weeks (n = 12–32)

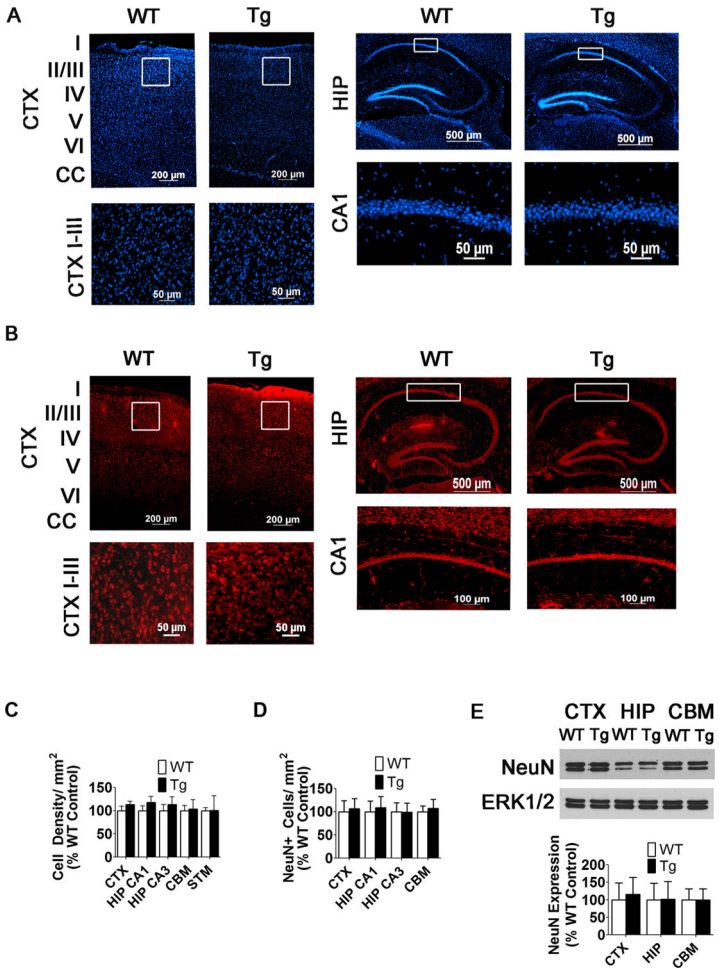

Fig. 3.

NeuN staining and DAPI density are not significantly changed in the CTX or HIP of 10-week-old male MeCP2-Tg mice. **a, b** No change in DAPI density or NeuN immunostaining in the CTX and HIP of 10-week-old WT and MeCP2-Tg mice ($n = 6$). Low-magnification images (top panels) and high-magnification images (bottom panels). White boxes in low-magnification images denote where high- magnification images are located. **c** Quantification of cell density in the CTX, HIP, CBM, and STM of 10-week-old WT and MeCP2-Tg mice ($n = 6$). **d** Quantification of NeuN+ cells in the CTX, HIP, and CBM of 10-week-old WT and MeCP2-Tg mice ($n = 6$). **e** Western blot analysis from CTX, HIP, and CBM of 10-week-old mice. ERK1/2 was used as a loading control. Top panel shows representative blot and bottom panel is quantification from multiple blots ($n = 6$)

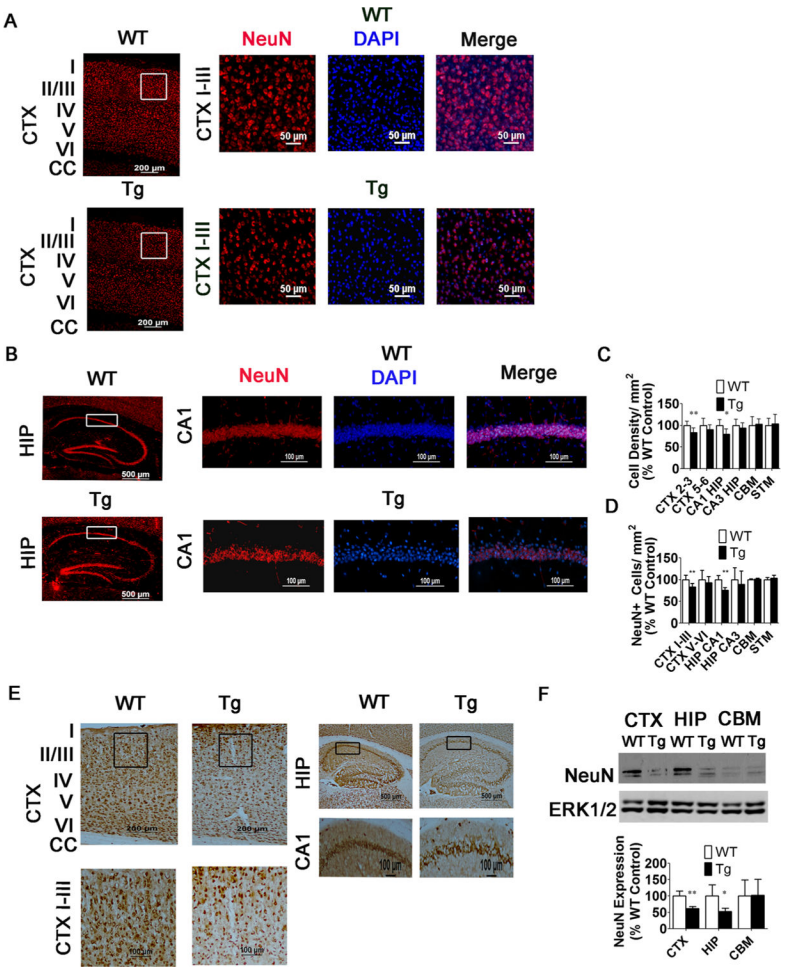

Fig. 4.

Reduction in NeuN+ cells and DAPI density in the CTX and HIP of 15-week-old MeCP2-Tg mice. **a, b** NeuN immunostaining in the CTX (a) and HIP (b) of 15-week-old WT and MeCP2-Tg mice. Left panel represents low- magnification image, and right panels represent higher-magnification images. The white box in the low-magnification image denotes location of higher-magnification image. **c** Quantification of DAPI density in the CTX, HIP, and CBM of 15-week-old WT and MeCP2-Tg mice ($n = 10$). **d** Quantification of NeuN+ cells in the CTX, HIP, and CBM of 15-week-old WT and MeCP2-Tg mice ($n = 10$). **e** NeuN DAB staining in the CTX and HIP of 15-week-old WT and MeCP2-Tg mice ($n = 7$). Low-magnification images (top panels) and high-magnification images (bottom panels). Black box in low-magnification images denotes location of higher-magnification image. **f** Western blot analysis from CTX, HIP, and CBM of 15-week-old mice WT and MeCP2-Tg mice. ERK1/2 was used as a loading control. Top panel shows representative blot and bottom panel quantification from multiple blots ($n = 7$)

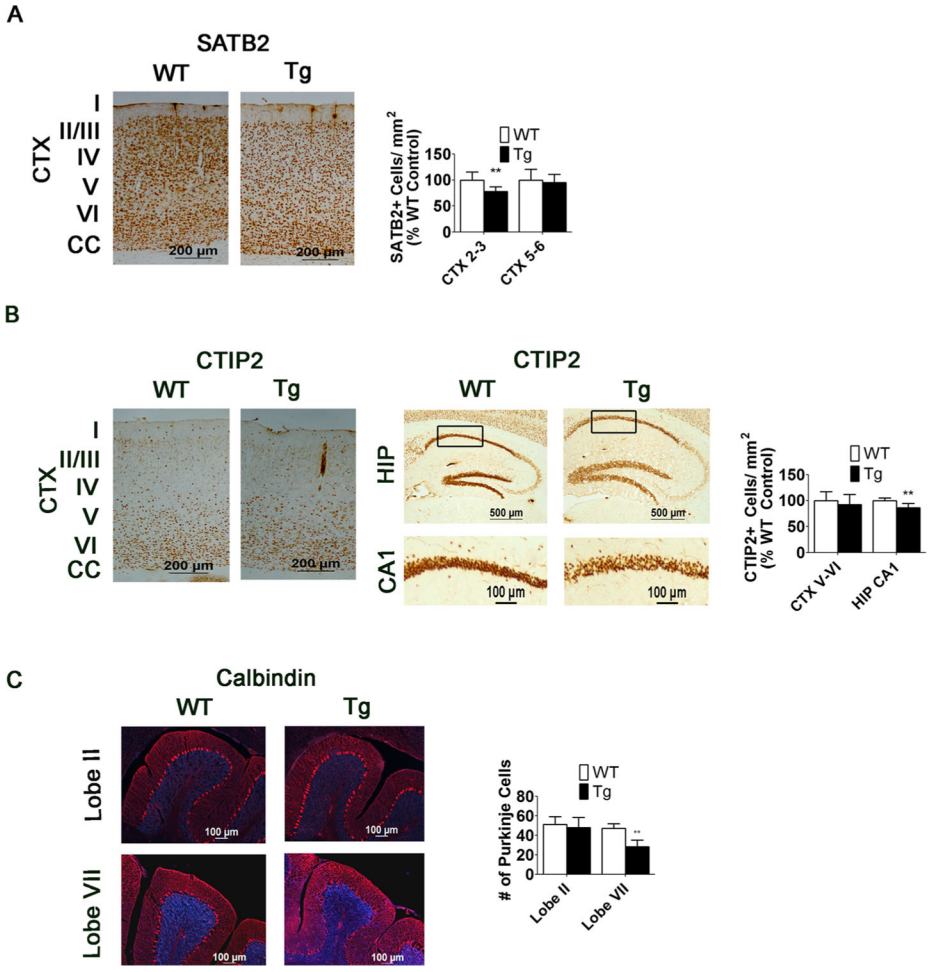

Fig. 5.

SATB2 and CTIP2 immunochemistry confirm reduction in neuronal numbers in 15-week-old MeCP2-Tg mice, and calbindin staining shows a loss of Purkinje cells in the CBM. a SATB2 immunoreactivity detected by DAB staining and SATB2-positive cell counts in the upper and lower layers of the CTX of 15-week-old WT and MeCP2-Tg mice ($n = 9$). **b** CTIP2 immunoreactivity detected by DAB staining and CTIP2-positive cell counts in the lower layers of the CTX and CA1 HIP of 15-week-old WT and MeCP2-Tg mice ($n = 9$). For HIP, upper panels are lower-magnification images and lower panels are higher-magnification images. The black box in the lower-magnification images denotes locations of the higher-magnification images. **c** Calbindin staining in lobes II and VII of the cerebellum (lobe II $n = 4$, lobe VII $n = 6$)

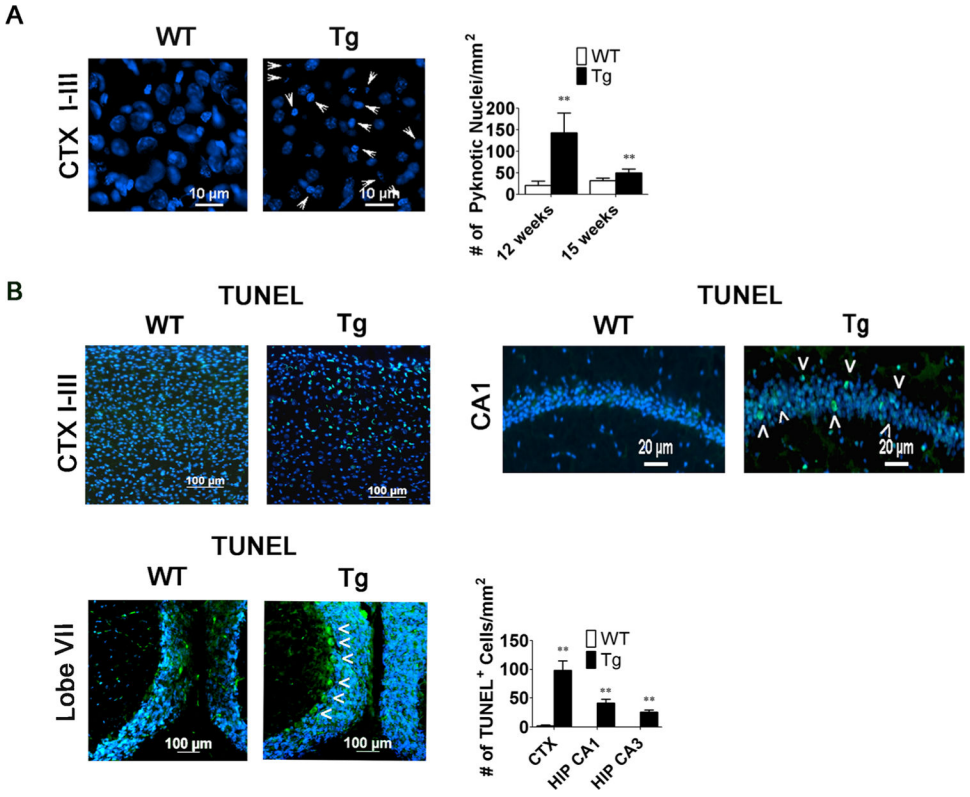

Fig. 6.

Neuronal loss in the MeCP2-Tg brain is apoptotic in nature. a Quantification of pyknotic appearing cells and measurement of cell width in the upper layers of the CTX of 12- and 15-week-old WT and MeCP2-Tg mice (12 weeks, $n = 4$ and 15 weeks, $n = 6$). Arrowheads indicate pyknotic nuclei. **b** TUNEL staining in the upper layers of the CTX, CA1 HIP, CBM, and STM and quantification of TUNEL-positive cells in the CTX and HIP of 12-week-old WT and MeCP2-Tg mice ($n = 4$). Arrowheads indicate TUNEL-positive cells

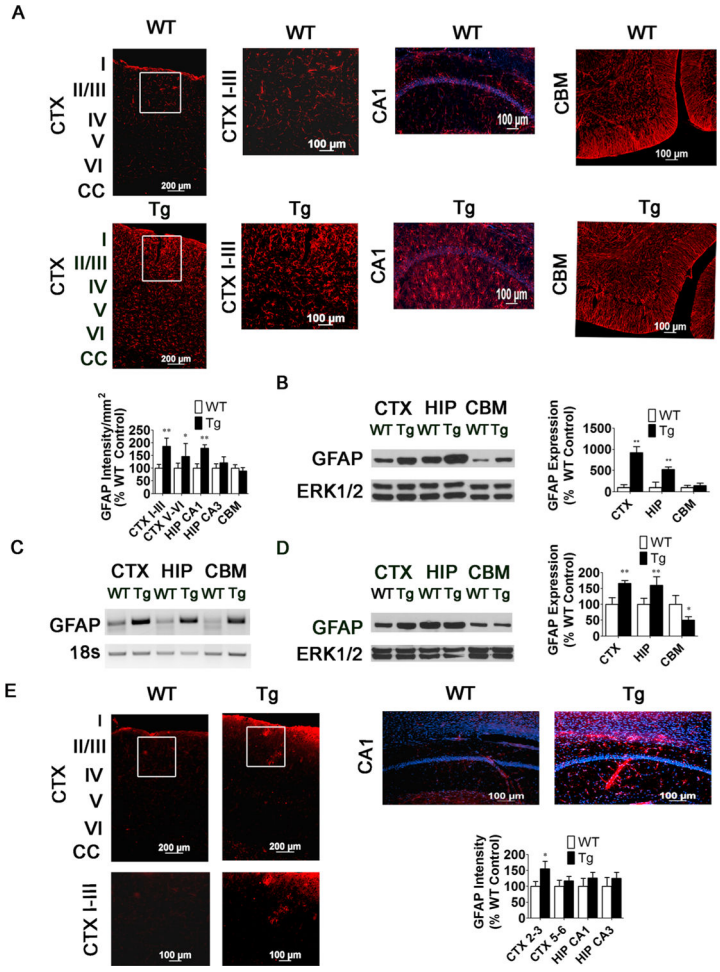

Fig. 7.

Increase in GFAP expression in MeCP2-Tg brain precedes neuronal loss but occurs in the same regions that subsequently display neuronal loss. **a** GFAP staining and measurement of staining intensity in the CTX, HIP, and CBM of 15-week-old WT and MeCP2-Tg mice (n = 9). CTX shows low- magnification image (left panels) and high-magnification images (right panels). The white box in low-magnification image denotes location of high-magnification image. **b** Western Blot and quantification showing expression of GFAP in CTX, HIP, and CBM of 15-week-old WT and MeCP2-Tg mice (n = 7). **c** GFAP RT-PCR in the CTX, HIP, and CBM of 15-week-old Tg mice. Eighteen seconds was used to normalize cDNA. **d** Western Blot and quantification showing expression of GFAP in the CTX, HIP, and CBM of 10-week-old WT and MeCP2-Tg mice (n = 5). ERK1/2 serves as a loading control. **e** GFAP staining and measurement of staining intensity in the CTX, HIP, and CBM of 15-week-old WT and MECP2-Tg mice (n = 6). For CTX, upper panels are lower-magnification images and lower panels are higher-magnification images. The white box in the lower-magnification images denotes locations of the higher-magnification images

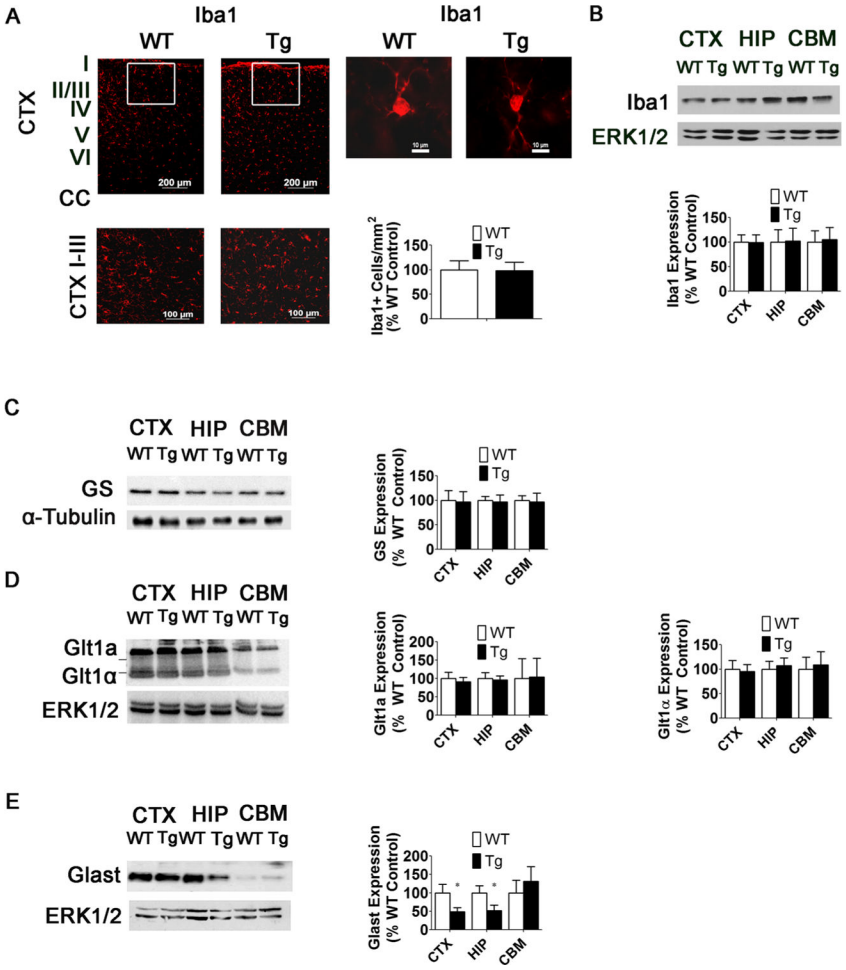

Fig. 8.

Increases in GFAP expression are not associated with a neuroinflammatory response. **a** Iba1 immunostaining and quantification in the CTX of 15-week-old WT and MeCP2-Tg mice (*n* = 5). Right panels, high-magnification image of single Iba1+ cell in 15-week-old WT and MeCP2-Tg mouse. b Western blot analysis of Iba1 expression and quantification in the CTX, HIP, and CBM of 15-week-old WT and MeCP2-Tg mice. Top panel is representative western blot and bottom panel is quantification of western blots (*n* = 3). **c** Western blot of glutamine synthetase (GS) expression and quantification of expression in the CTX, HIP, and CBM of 15-week-old WT and MeCP2-Tg mice. α-Tubulin was used as a loading control rather than total ERK1/2 because the molecular weight of GS overlaps with the molecular weight of total ERK1/2 (*n* = 3). **d** Western blot of Glt1 expression and quantification of Glt1 expression in the CTX, HIP, and CBM of 15-week-old WT and MeCP2-Tg mice (*n* = 3). **e** Western blot of Glast expression and quantification of Glast expression in the CTX, HIP, and CBM of 15-week-old WT and MeCP2-Tg mice (*n* = 3)

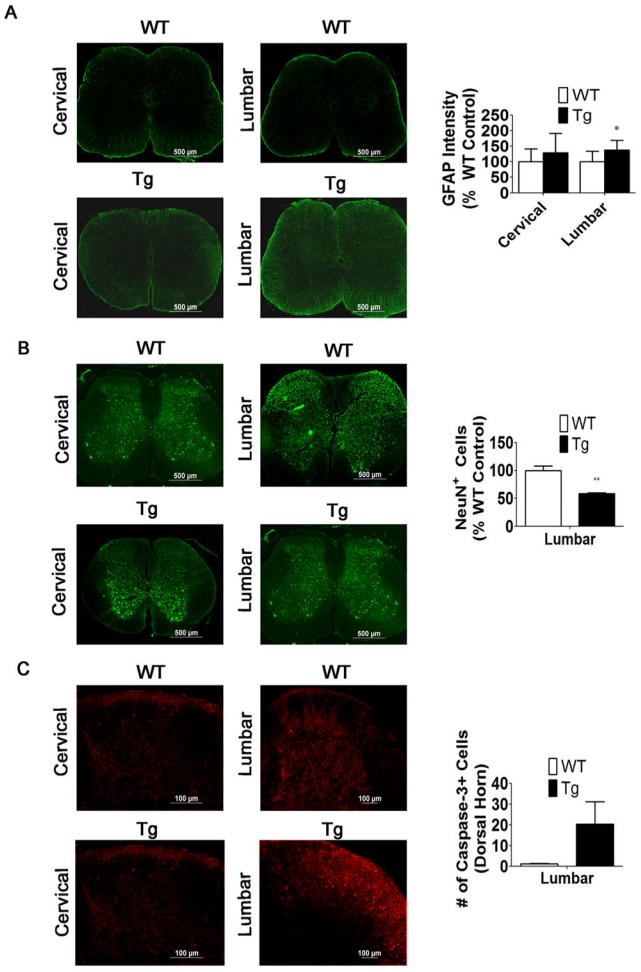

Fig. 9.

Increased GFAP staining and caspase-3+ cells correlates with a reduction in NeuN+ cells in the lumbar spinal cord. **a** GFAP staining and measurements of staining intensity in the cervical and lumbar spinal cord of 6- week-old WT and MeCP2-Tg mice ($n = 4$). **b** NeuN immunostaining and quantification of NeuN+ cells in the lumbar spinal cord of 6-week-old WT and MeCP2-Tg mice ($n = 4$). Since changes in the number of DAPI-stained cells could contribute to the changes in number of NeuN-positive cells, positive cell counts were normalized to DAPI and expressed as a percentage of wild-type littermate controls. **c** Capase-3+ cells are increased in the lumbar region of the spinal cord of 6-week-old MeCP2-Tg mice compared to the WT ($n = 4$)

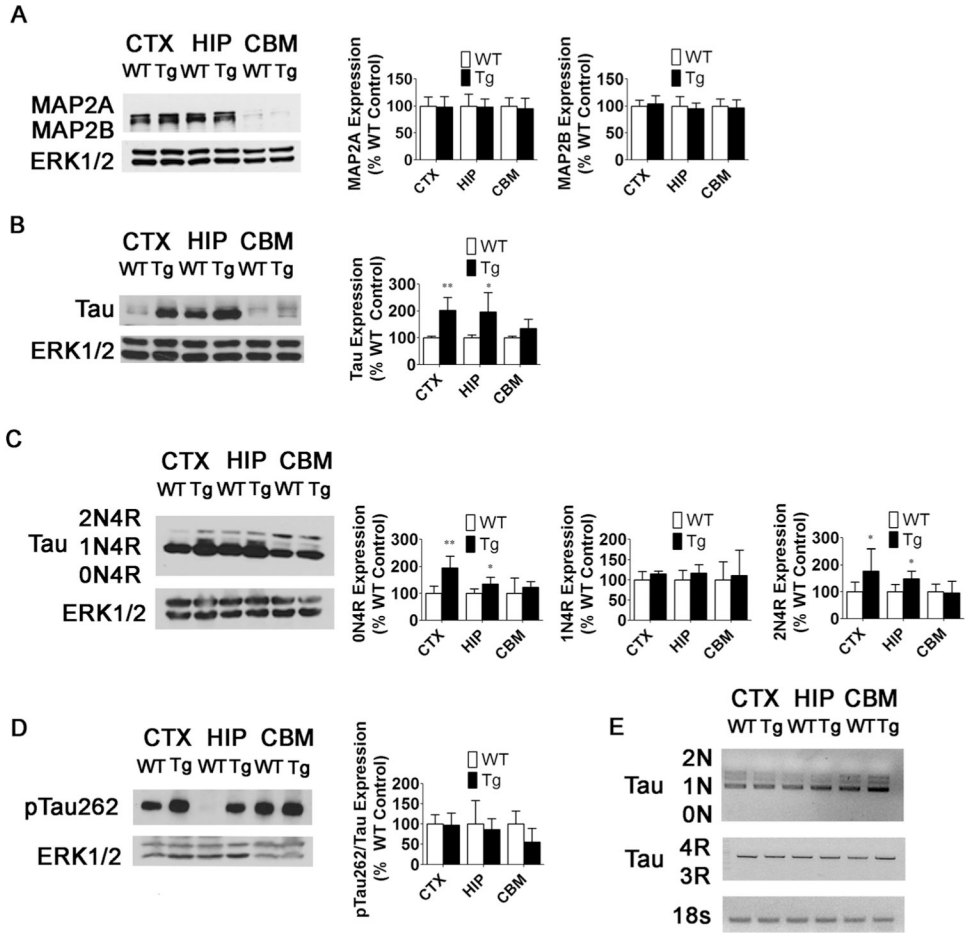

Fig. 10.

Expression of Tauprotein, but not mRNA, is increased in 15-week-old MeCP2-Tg mice. **a** MAP2 expression and quantification in the CTX, HIP, and CBM of 15- week-old WT and MeCP2-Tg mice ($n = 3$). **b** Total Tau expression and quantification in the CTX, HIP, and CBM of 15- week-old WT and MeCP2-Tg mice ($n = 5$). **c** Tau isoform expression and quantification in the CTX, HIP, and CBM of 15-week-old WT and MeCP2-Tg mice ($n = 5$). **d** Ratio of pTau262 to total Tau in the CTX, HIP, and CBM of 15-week-old WT and MeCP2-Tg mice ($n = 5$). **e** Tau isoform RT-PCR in the CTX, HIP, and CBM of 15-week-old MeCP2-Tg mice. Eighteen seconds was used to normalize cDNA ($n = 3$)

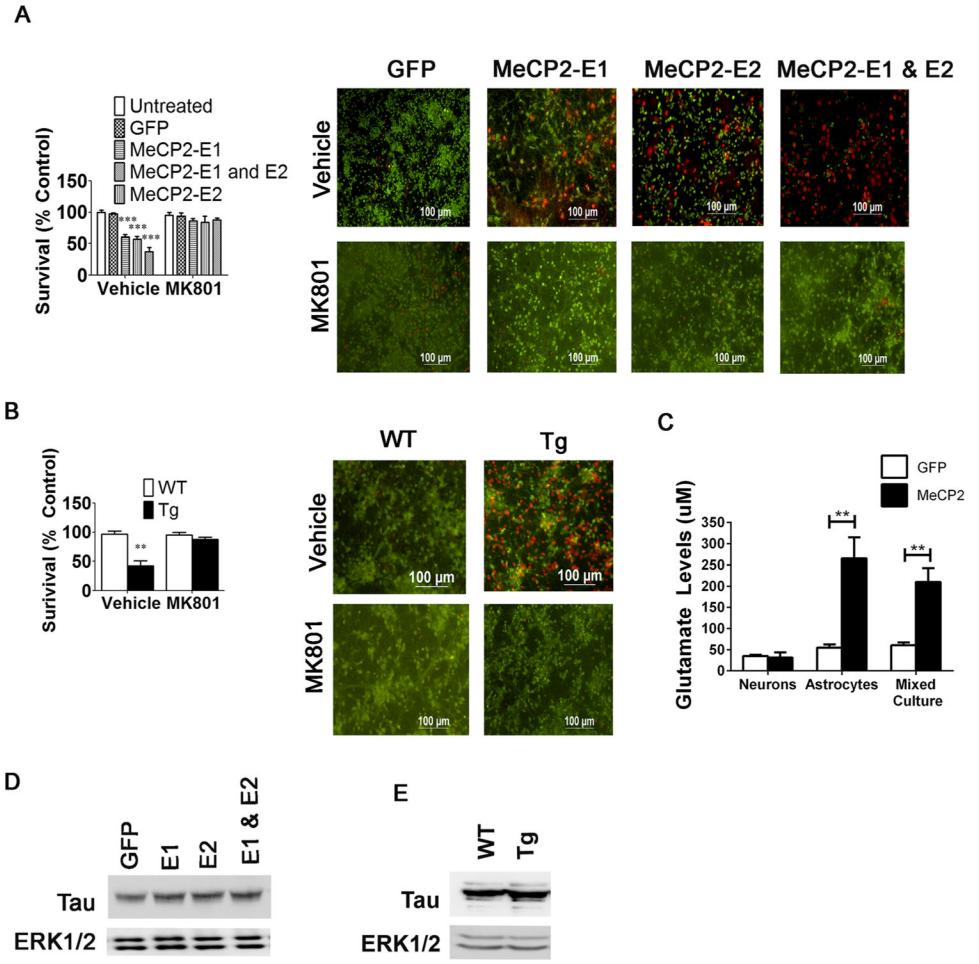

Fig. 11.

Conditioned media from cortical astrocytes infected with MeCP2 adenovirus and conditioned media from cortical astrocytes from male MeCP2-Tg mice kills cortical neurons. **a, b** Pretreatment with an NMDA receptor antagonist, MK801 (1 μM), prevents astrocyte conditioned media from killing cortical neurons ($n = 3$). **c** Glutamate levels are increased in the media of pure astrocyte cultures or mixed neuronal + astrocyte cultures overexpressing MeCP2, but not pure neuronal cultures overexpressing MeCP2. **d** Tau expression is increased in cortical neurons after treatment with astrocyte conditioned media from astrocytes overexpressing MeCP2 ($n = 2$). **e** Tau expression is increased in cortical neurons after treatment with astrocyte conditioned media from male WT or MeCP2-Tg mice ($n = 2$)

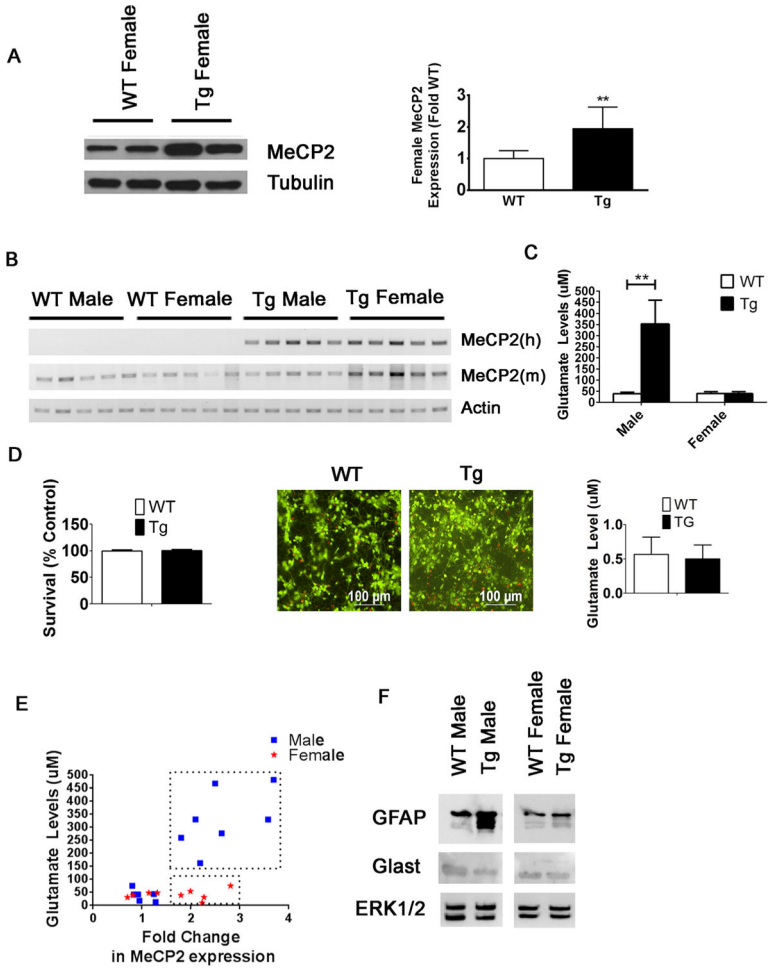

Fig. 12.

Conditioned media from MeCP2-Tg female cortical astrocytes does not kill cortical neurons. **a** Left panel shows representative Western blot of MeCP2 expression in the cortex of two WT and two MeCP2-Tg 15-week female mice. Alpha tubulin was used as a loading control. Right panel shows quantification of 15-week WT ($n = 8$) and MeCP2-Tg ($n = 9$) female cortical lysates. **b** RT-PCR analysis of the cortex of male and female WT and MeCP2-Tg mice using primers human (h) and mouse (m) MeCP2 ($n = 5$). **c** Glutamate homeostasis is affected in male MeCP2-Tg mice but not in female MeCP2-Tg mice ($n = 3$). **d** Conditioned media from MeCP2-Tg female cortical astrocytes does not affect cortical neuron survival ($n = 3$), and there is no significant change in glutamate levels in conditioned media from WT and MeCP2-Tg female astrocytes ($n = 3$). **e** MeCP2-Tg males display elevated glutamate levels with increased MeCP2 expression($n = 7$), while MeCP2-Tg females do not ($n = 5$). Transgenic animals are denoted in boxes. f Increased GFAP expression and decreased GLAST in male, but not female, MeCP2-Tg mice. ERK 1/2 was used as a loading control

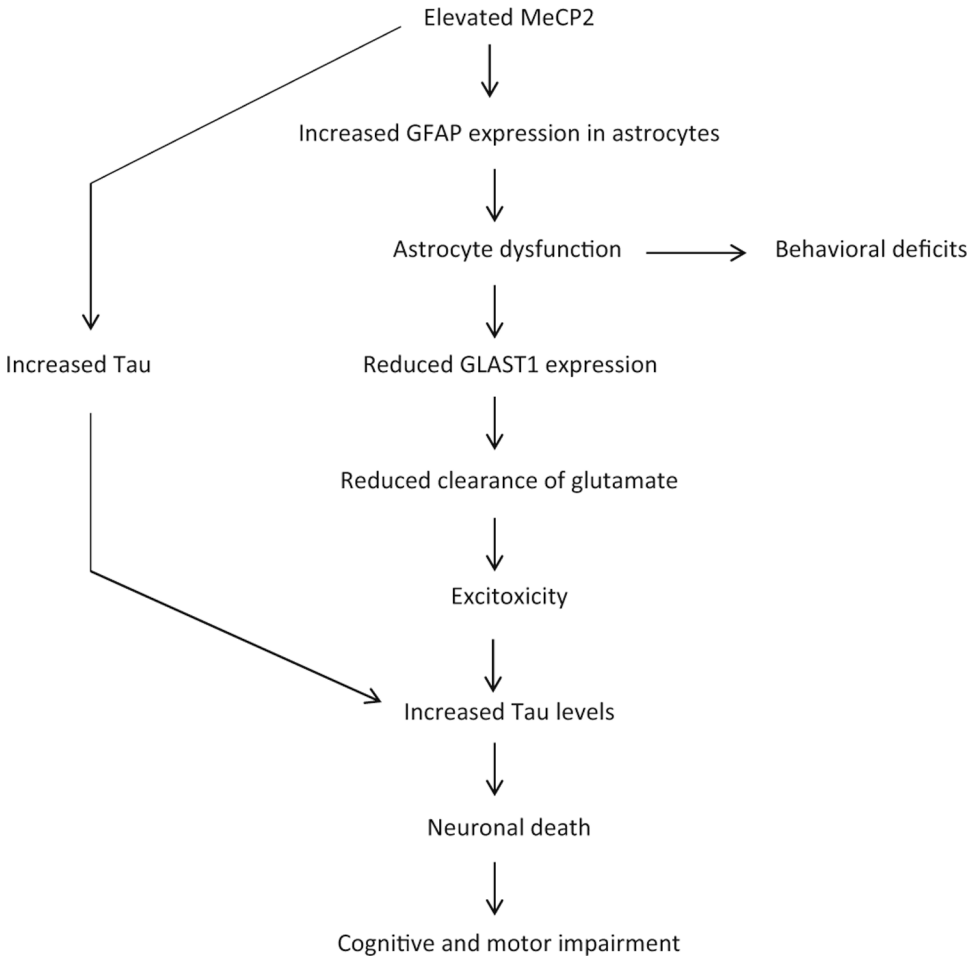

Fig. 13.

Model for MeCP2 triplication syndrome. Elevated MeCP2 resulting from gene duplication/triplication leads to an upregulation of GFAP expression in the cortex and hippocampus, which along with a downregulation of GLAST1 results in dysfunction of astrocytes. The reduced GLAST1 affects glutamate clearance thus promoting excitotoxicity, which increases levels of Tau. The effects of elevated Tau along with excitotoxicity cause the death of cortical and hippocampal neurons. Increased Tau could also result from the high expression of MeCP2 in neurons. The loss of neurons in the cortex, hippocampus, and cerebellum result in severe cognitive and behavioral deficits, seizures leading to premature death